SCIENCE CHINA
Technological Sciences

Special Topic: Digital Image Correlation
• Review •

January 2018 Vol.61 No.1: 2–20
https://doi.org/10.1007/s11431-017-9090-x

Review of single-camera stereo-digital image correlation techniques for full-field 3D shape and deformation measurement

PAN Bing[1*], YU LiPing[1] & ZHANG QianBing[2]

[1] *Institute of Solid Mechanics, Beihang University, Beijing 100191, China;*
[2] *Department of Civil Engineering, The University of Hong Kong, Hong Kong, China*

Received April 24, 2017; Accepted June 28, 2017; published online September 12, 2017

Single-camera stereo-digital image correlation (stereo-DIC) techniques have gained increasing attentions and demonstrated excellent prospects in the experimental mechanics community owing to their prominent advantages of cost-effectiveness, compactness, and the avoidance of the complicated camera synchronization. Using additional optical devices, e.g. a diffraction grating, a bi-prism or a set of planar mirrors, pseudo stereo images of a test sample surface can be recorded with a single camera. By correlating these stereo images using DIC, full-field three-dimensional (3D) shape and deformation can be retrieved. This review comprehensively summarizes the historical development, methodologies, strengths and weaknesses of the diffraction grating-based, prism-based, four-mirror-adaptor-based single-camera stereo-DIC techniques, and the recently proposed novel full-frame single color camera-based stereo-DIC technique for full-field 3D shape and deformation measurement. The optical arrangements, principles and calibration procedures of these single-camera stereo-DIC techniques are described in detail. Since high-speed deformation measurement is efficiently achieved by combining the single-camera stereo-DIC with one high-speed camera, single-camera stereo-DIC techniques show great potential in impact engineering, vibration and other dynamic tests.

single-camera stereo-DIC, diffraction grating, bi-prism, four-mirror adapter

Citation: Pan B, Yu L P, Zhang Q B. Review of single-camera stereo-digital image correlation techniques for full-field 3D shape and deformation measurement. Sci China Tech Sci, 2018, 61: 2–20, https://doi.org/10.1007/s11431-017-9090-x

1 Introduction

Stereo- or three-dimensional (3D) digital image correlation (stereo-DIC or 3D-DIC) using two synchronized digital cameras has been convincingly proven to be a powerful and versatile non-contact optical technique for full-field 3D shape, motion and deformation measurements in the field of experimental mechanics [1–7]. In this review, to maintain the consistent, the terminology of stereo-DIC is used. Compared with its 2D counterpart (i.e., 2D-DIC) using a single camera, which can merely measure the in-plane deformation of nominal planar objects [8], stereo-DIC is more practical and powerful since it applies to 3D shape and deformation measurements of both planar and curved surfaces. More specifically, stereo-DIC provides more accurate measurements than 2D-DIC, because it simultaneously measures three displacement components, rather than being affected by out-of-plane displacements [9,10].

Nevertheless, in practical applications, the requirement of two synchronized cameras usually makes the construction of a regular binocular stereo-DIC system both expensive and complicated, especially in the cases of measuring transient deformation using two high-speed or ultra-high-speed cameras [11]. In these cases, the need of using two synchronized high-speed cameras not only greatly increases the hardware cost but also involves complexity on the synchronization of

*Corresponding author (email: panb@buaa.edu.cn)

two high-speed cameras [12,13]. Moreover, the requirement for two cameras often limits their application due to experimental constraints or physical camera constraints [12]. In addition, the nonlinear geometric distortions and intensity variations between the image pairs, which are acquired by two different cameras with different optical properties and orientations, may inevitably result in difficulty in achieving precise stereo matching and thus decrease measurement accuracy [14]. These limitations stimulate the necessity for the development of alternative stereo-DIC methods that solely use one camera.

Inspired by the basic laws of optics, numerous single-camera stereovision techniques, including diffraction grating-based, prism-based and mirror-based approaches, have been established in the field of machine vision and optical imaging by incorporating a diffraction grating, a prism or a set of planar mirrors. With the aids of these additional optical devices, the incoming scene is equally split into two sub-images or diffracted into two diffraction images projecting at different angles on the camera sensor. These sub-images could be considered as a pseudo stereo image pair recorded from two different orientations by two virtual cameras. Recently, these single-camera stereovision techniques have been successfully combined with DIC for 3D shape and deformation measurements. For instance, Xia et al. [15] proposed a transmission diffraction grating-based single-camera stereo-DIC method for 3D displacement measurement of a small soft membrane. Genovese et al. [13] established a bi-prism based single-camera stereo-DIC system and verified its accuracy for 3D shape and deformation measurement. Pankow et al. [12] combined a four-mirror adapter-assisted single-camera stereovision system with DIC and successfully measured the out-of-plane deformations of an aluminium plate under a shock wave impact. More recently, a novel color stereo-DIC method using a single three charge-coupled device (3CCD) color camera was proposed by the authors of this paper for 3D shape and deformation measurement [16]. Compared with other single-camera stereo-DIC methods, this newly presented approach enables two images of the object surface to overlap each other via different color channels, which ensures the full application of the spatial resolution of the camera sensor for obtaining 3D information.

Although plenty of literature regarding single-camera stereo-DIC techniques have been published recently, a comprehensive review covering the historical development, basic principles, fundamental technical details, as well as strengths and limitations of these techniques is still lacking. Considering the attractive benefits of single-camera stereo-DIC techniques and their great potential in certain cases (e.g., measuring transient 3D deformation using a single high-speed camera, retrieving 3D deformation through constrained optical configuration), the thorough understanding of these techniques is undoubtedly beneficial to properly selection and optimal use of a single-camera stereo-DIC technique. To this end, this paper comprehensively reviews the current grating-based, prism-based and mirror-based single-camera stereo-DIC techniques. The historical overview, technical specifications (including optical arrangement, principles and calibration) and their strengths and limitations are systematically presented and discussed.

2 Diffraction grating-based single-camera stereo-DIC methods

2.1 Historical overview

Trivi and Rabal [17] proposed the earliest grating-based single-camera stereovision technique, and demonstrated that a diffraction grating was a useful tool to identify a stereoscopic pair of an object within a single exposure under monochromatic illumination. As shown in Figure 1, a diffraction grating is vertically placed between the lens and the test object, and is aligned to be perpendicular to the optical axis of the imaging system. Then, the object is illuminated through a quasi-monochromatic light source instead of the conventional white light source, since the recorded images are significantly affected by the chromatic dispersion. As a result, high-order (i.e., positive and negative first-order) diffraction images P_{+1} and P_{-1} of the object appear symmetrically replicated on the ordinary (zero-order) image P_0. Note that these twin diffraction images produced by closer objects are less dispersed than those produced by far-away objects. By analyzing the optical model according to the diffraction theory, the distance between the zero-order and first-order diffraction images can be deduced as [17]

$$d = \frac{\lambda f_0 L_1 L_3}{L_1 + L_2}, \tag{1}$$

where λ denotes the wavelength of the illumination light, f_0 is the frequency of the grating, L_1, L_2 and L_3 are the distances defined in Figure 1.

Inspired by this grating-based single-camera stereovision technique, the feasibility of 3D deformation measurement by adding a diffraction grating to the Burch experimental setup was explored by Henao et al. [18]. The 3D displacement components on the object surface were carefully derived based on the projection relationships. Ordinarily, the derived equations require a precise determination of the different distances involved. These distances may be obtained by measuring the distances between the principal planes of the optical components. An alternative method to determine all the instrumental constants can be achieved by calibrating the optical system through rigid-body translations. Moreover, Rabal et al. [19] reported a digital speckle pattern shearing interferometer with the assistance of a diffraction grating as a shearing element. A diffraction grating took the placement of

Michelson interference devices, which resulted in a relatively compact optical setup.

Xia et al. [15] combined the diffraction grating-based single-camera stereovision with 2D-DIC for measuring full-field 3D deformation [20], however this method can only be utilized to measure 3D deformation of transparent planar samples. Pan and Wang [21] recently found that the assumed optical imaging model, mathematical derivations and final formulas are not sufficiently rigorous, which may lead to significant measurement errors, particularly within the out-of-plane displacement component. Based on a simple but practical pinhole imaging model, theoretical formulas for reconstructing the profile and measuring 3D displacements of the object surface were modified, and proven to be effective and accurate upon measuring 3D deformation of an adhesively bonded single lap joint (SLJ) (Figure 2) [22]. Thereafter, Xia et al. [23] developed a novel optical microscope system for full-field 3D shape and deformation measurements by integrating the diffraction-assisted DIC with the fluorescent microscopy. Regardless of these developments and applications, it should be noted that the diffraction assisted stereo-DIC system is limited to small objects in a size varying from sub-millimeters to a few centimeters due to the size constraints of the diffraction grating.

2.2 Optical arrangement

Figure 3 shows a typical optical arrangement of the grating-based single-camera stereo-DIC method for 3D shape and

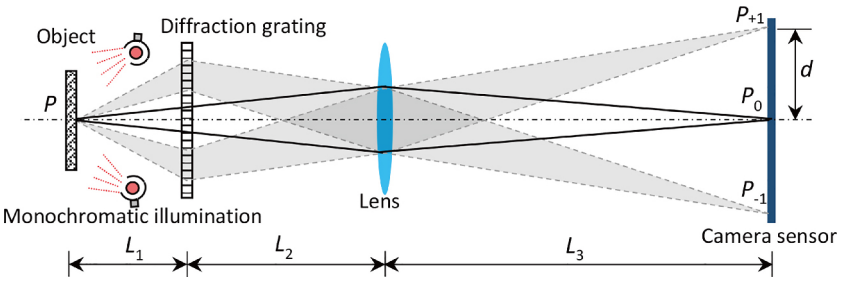

Figure 1 (Color online) Schematic diagram of the single-camera stereovision system using a diffraction grating.

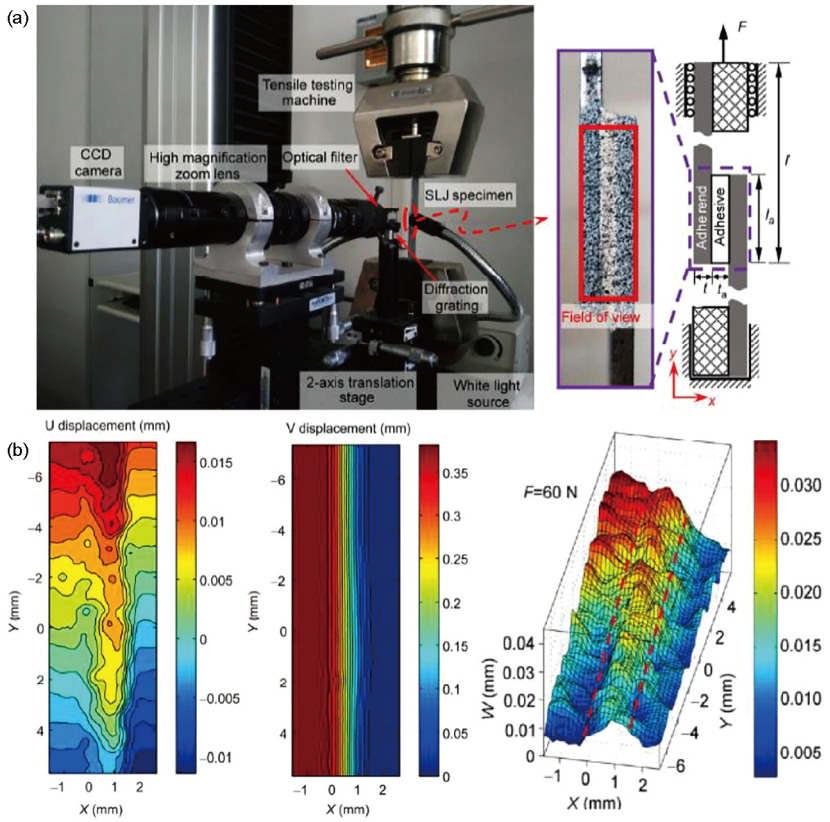

Figure 2 (Color online) (a) Experimental setup with a close-up and schematic geometry of SLJ specimen; (b) measured *U*, *V* and *W* displacement fields of the SLJ specimen under the load of 60 N (Pan et al. [22]).

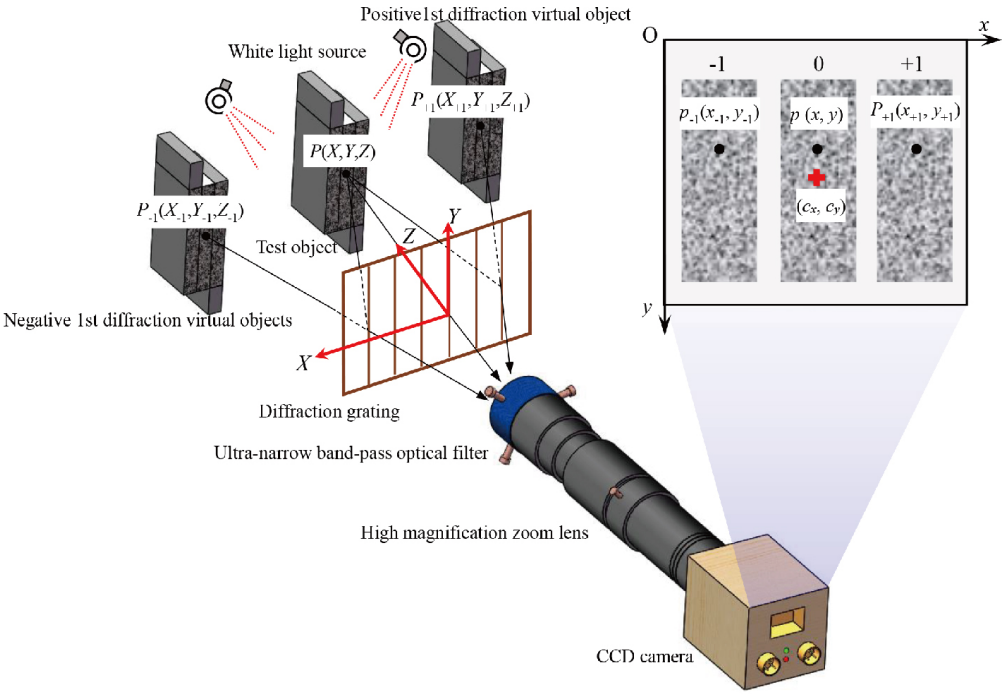

Figure 3 (Color online) Improved optical arrangements of the single-camera stereo-DIC method using a diffraction grating (Pan and Wang [21]).

deformation measurement. This system is composed of a digital CCD/complementary metal oxide semiconductor (CMOS) camera, a camera lens, a transmission diffraction grating and a quasi-monochromatic light source. Similar as the early reported diffraction assisted single-camera stereo-imaging technique [17], the diffraction grating is symmetrically positioned between the lens and the test object. By adjusting the distances among the camera lens, the diffraction grating and the object and illuminating the object using a monochromatic light source, the zero-order, the positive and negative first-order diffraction images of the object are recorded by the camera. Note that, whether in work by Xia et al. [15] or the improved work by Pan and Wang [21], the specimens were both illuminated by a quasi-monochromatic light. Whilst experiments are conducted in a darkroom, the different ambient light may introduce adverse impact (e.g., chromatic dispersion) onto the recorded images. To address this problem, an effective approach proposed by Pan et al. [22] outfits an ultra-narrow bandpass optical filter before the zoom lens and illuminates the specimen with white light sources instead of using the quasi-monochromatic source (Figure 3). The ultra-narrow bandpass optical filter allows only quasi-monochromatic light within its limited wavelength range to pass through, and thus can skillfully suppress the potential adverse impact of varying ambient light and also make the system relatively compact. As shown in Figure 3, the positive and negative first-order diffraction images are the desired stereo image pair that encodes 3D geometric information, located on each side of the zero-order diffraction image. By processing the positive and negative first-order diffraction images, the full-field profile and 3D deformation on the specimen can be obtained.

2.3 Principles

The 3D shape can be commonly retrieved by a pair of images of the test object using the conventional stereo-DIC algorithm. However, as the imaging model of the grating-based single-camera stereo-DIC system is greatly different from that of a conventional stereo-DIC system, significant errors will be introduced into measuring results if using a traditional stereo-DIC algorithm. Therefore, to accurately determine 3D shape and deformation from the recorded diffraction images, the imaging model of the grating-based single-camera stereo-DIC system should be initially established. As shown in Figure 3, a coordinate system is established with its origin O (0, 0, 0) located at the intersecting point of the optical axis and the diffraction grating. With this coordinate system, the real coordinate of a point on the test object surface is denoted as $P(X, Y, Z)$. Then, the coordinates of corresponding two first-order diffracted points are represented by $P_{-1}(X_{-1}, Y_{-1}, Z_{-1})$ and $P_{+1}(X_{+1}, Y_{+1}, Z_{+1})$, respectively. Assuming the corresponding image coordinates of these three points are $p(x, y)$, $p_{-1}(x_{-1}, y_{-1})$ and $p_{+1}(x_{+1}, y_{+1})$, respectively, it is necessary to establish mathematical relationships between the real coordinates and image coordinates to reconstruct the 3D coordinates of the test object. Based on the backward ray-tracing method, the diffraction theory and the ideal pinhole camera model, the real 3D coordinates of a point can be derived and

written as [21]

$$X = -\frac{(x_{+1}+x_{-1}-2c_x)}{2M},$$
$$Y = \frac{(y_{+1}+y_{-1}-2c_y)}{2M}, \quad (2)$$
$$Z = \frac{(x_{+1}-x_{-1})}{2M\tan\theta},$$

where (c_x, c_y) is the center of the recorded image; M=$L_{\text{img}}/(Z_{\text{obj}}\times P_{\text{sz}})$ is the magnification factor of the optical system, which is assumed as a constant and needs to be calibrated; L_{img} and Z_{obj} are the image and object distances of the optical system, respectively; P_{sz} is the pixel size of the camera; θ=$\sin^{-1}(\lambda/p)$ the first-order diffraction angle with λ being the wavelength of the quasi-monochromatic light source and p denoting the pitch of the grating.

As shown in Figure 4, the image coordinates (i.e., (x_{+1}, y_{+1}) and (x_{-1}, y_{-1})) correspondence of two diffracted points are obtained by matching the positive first-order and the negative first-order diffraction images of the test specimen using the well-established subset-based 2D-DIC algorithm. Once the image coordinates of two diffracted points and the magnification factor are determined, the 3D coordinates of the test specimen can be obtained.

Then, based on the pinhole imaging model and some approximations, Pan and Wang [21] derived three displacement components of the measurement point $P(X, Y, Z)$ as

$$U \cong -\frac{u_{+1}+u_{-1}}{2M},$$
$$V \cong \frac{v_{+1}+v_{-1}}{2M}, \quad (3)$$
$$W \cong \frac{u_{+1}-u_{-1}}{2M\tan\theta}\left(\frac{Z_{\text{obj}}}{Z_{\text{obj}}-Z}\right),$$

where u_{+1} and v_{+1} are the x- and y-directional displacements of the positive first-order diffracted images, respectively; u_{-1} and v_{-1} are the x- and y-directional displacements of the negative first-order diffracted images, respectively; Z is the distance of each measurement point to the grating, which can be achieved after shape reconstruction.

2.4 Calibration of the imaging system

As presented in the final formulas given in eqs. (2) and (3), to determine the profile and 3D deformation of the test specimen, the magnification factor M and the object distance Z_{obj} must be calibrated in advance. Pan and Wang [21] performed in-plane and out-of-plane translations to determine these two parameters. By fitting actual displacements with the measured displacement or average normal strains using linear least squares, the magnification factor M and the object distance Z_{obj} can be accurately calibrated.

In addition, in the grating-based single-camera stereo-DIC system, image distortions may unavoidably exist due to imperfections of the diffraction grating, lens distortion and non-uniform spatial distribution of the sensing pixels. Moreover, the misalignment between the diffraction grating and camera also will alter the image model of the imaging system and further decrease its measurement accuracy. In specific cases, these image distortions may introduce considerable measuring errors into results. To achieve a high-accuracy shape and 3D deformation measurement, these distortions should be calibrated and eliminated as possible. Note that, as indicated in ref. [20], the image distortion caused by the imperfection of the diffraction grating is negligible. Thus, lens distortion, non-uniform spatial distribution of the sensing pixels and the misalignment between the diffraction grating and camera need to be calibrated. In ref. [20], a non-parametric

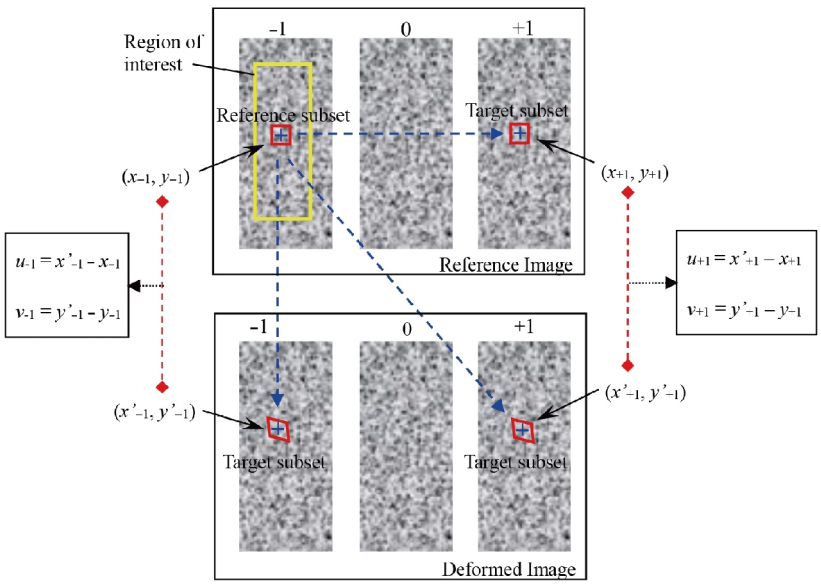

Figure 4 (Color online) Calculation of image displacements for profile and 3D displacement measurement using 2D-DIC (Pan and Wang [21]).

method of distortion calibration was used to determine the combined lens and sensor distortion in the established system.

3 Prism-based single-camera stereo-DIC methods

3.1 Historical overview

The prism-based single-camera stereovision technique was originally proposed in computer vision by Lee et al. [24] and Lee and Kweon [25]. In their work, a bi-prism stereo projection matrix was devised to characterize the relationship between an object point and its two virtual points, and a ray tracing method was used to calculate the projection from the object point to its image points. As shown in Figure 5(a), a bi-prism is vertically placed between the lens and the test object. With the aid of the bi-prism, an arbitrary point on the object is transformed into two virtual points. Stereo image pairs are therefore imaged onto the left and right halves of the real camera sensor attributable to the refraction of light rays. Differing from Lee's virtual point concept, a new understanding of the single-camera stereovision system was later proposed by Lim and Xiao [26]. As indicated in Figure 5(b), it was assumed that the stereo image pair acquired by the established single-camera system was equivalent to the two images simultaneously obtained by two virtual cameras. Thereafter, a series of studies on the bi-prism-based single-camera system, including system construction [27–29], parameter error analysis [30], system calibration [31], and stereo correspondence matching [32,33], were conducted by Lim's group. It is postulated that image distortions were negligible in these studies. However, unlike standard stereovision systems using two or more independent cameras whose distortions (primarily lens distortions) might not be severe, or could be evaluated and easily eliminated, the distortion induced by the prism in front of the camera always exist, even within an ideal system setup. To resolve this problem, a parametric bi-prism distortion model [34] and a fully constrained and model-free distortion correction method [35,36] for the single-lens stereovision system using a bi-prism were proposed.

In addition to the bi-prism, the tri-prism and the multi-face prism also have been employed to establish single-camera stereovision systems. For example, Xiao and Lim [37] established a single-camera trinocular stereovision system using a single CCD camera and a pyramid-like tri-prism. This system can simultaneously capture three different views of the same scene and these views can be regarded as the images captured by a set of virtual cameras produced by the prism. Wang et al. [38] proposed a new method for the image rectification of a single-lens stereovision system with a tri-prism. This approach is based on geometry analysis of ray sketching and does not require the intricate calibration process. Accordingly, to develop a portable prism-based stereovision system

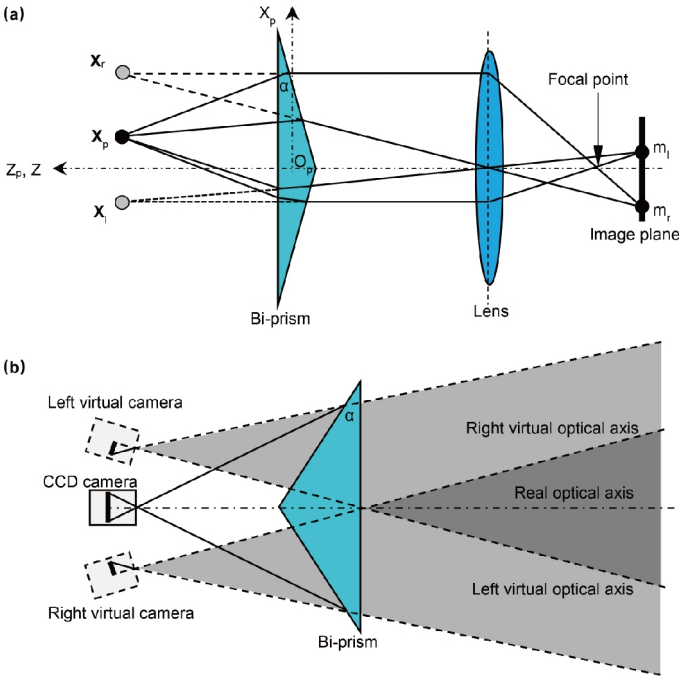

Figure 5 Schematic diagram of the single-camera stereovision system using a bi-prism: (a) virtual point concept (Lee and Kweon [25]); (b) virtual camera concept (Lim and Xiao [26]).

which has a smaller volume and lower weight, Chen et al. [39] designed a micro-prism array plate to replace the conventional prism. With this micro-prism plate, the established portable prism-based system can create stereo image pairs on the camera sensor. Recently, Yang et al. [40] reported a micro-prism array based compact stereo endoscopic camera with a single image sensor. This stereo endoscopic camera can split an image into two stereo images and successfully demonstrates the binocular disparities between the stereo image pairs for objects with different distances.

Inspired by the prism-based stereovision techniques developed in other fields, Genovese et al. [13] designed and validated a single-camera stereo-DIC system using a bi-prism for 3D deformation measurement. In their work, a model-free image distortion correction scheme was proposed to overcome the shortcomings related to the utilization of a thick prism and made it possible to perform high accuracy time-resolved 3D deformation measurements on an inflated latex membrane. Then, based on the principle of light refraction and a backward ray-tracing method, Wu et al. [41,42] modified the virtual point model and proposed a novel shape retrieval method to improve the accuracy of bi-prism aided single-camera stereo-DIC system. Compared with the original virtual point model, the modified model is somewhat objective since it does not require the assumption that the virtual points are symmetric regarding the object point.

Recently, an improved bi-prism-based single-camera stereo-DIC system using a bilateral telecentric lens was established by Wu et al. [43] to carefully eliminate the

systematic errors caused by manufacturing deficiency of the bi-prism and distortion of the bilateral telecentric lens [44]. With the unique design of the bilateral telecentric lens, the imaging model of the prism-based single-camera stereo-DIC system is greatly simplified and the complicated calibration process is prevented. The accuracy of this system was validated by experiments and proven to be more accurate than those using a conventional camera lens. The validity of various bi-prism-based single-camera stereo-DIC techniques has been demonstrated by measuring the shape of an aluminum cylinder (Figure 6), and 3D deformation of a circular latex membrane in an inflation test. Subsequently, by combining the idea of active imaging proposed by Pan et al. [45,46] with the bi-prism-based single-camera stereo-DIC technique, Wu et al. reported the measurement of high-temperature 3D deformation via a narrow and deep optical observation window of a high-temperature furnace [47].

3.2 Optical arrangement

The optical arrangements of the single-camera stereo-DIC system using a bi-prism and a conventional lens are schematically presented in Figure 7. Similar to the grating-based single-camera stereo-DIC method, a bi-prism is vertically placed between the camera and the object. With the aid of the bi-prism, two different views of the object are simultaneously imaged onto the two halves of the camera sensor after two refractions in the bi-prism. Consequently, the bi-prism-based single-camera stereo-DIC system can be recognized as a pseudo stereovision system using two virtual cameras. For an ideal perfectly aligned system, it is found that the exact position and orientation of two virtual cameras are determined as a function of the characteristics of the bi-prism (e.g., index of refraction and wedge prism angle) and the relative distances between the camera, bi-prism and the object [13]. The pan angle of the virtual-stereo system is directly related to wedge prism angle, while the lateral separation between two sub-images on two halves of the sensor depends on the relative distances among the camera, bi-prism and the object. Moreover, to suppress the chromatic aberration of the prism and realize a high-accuracy measurement, a monochromatic light source is required.

Differing from the bi-prism single-camera stereo-DIC system using a conventional lens, a simplified single-camera stereo-DIC system was established by Wu et al. [43] by combing a bilateral telecentric lens with a bi-prism. Upon using this system, light rays from the objects first deflect from the original optical path at the front surface of the wedge prism due to refraction, but directly pass through the interface of the back surface without changing direction. This significant difference in the imaging model can be attributed to the differences in imaging mechanisms between a bilateral telecentric lens and a conventional lens based on the pinhole model. As described in ref. [43], a mathematical model of the established single-camera stereo-DIC system was significantly simplified by using a bilateral telecentric lens. Although a high-quality bilateral telecentric lens has been recommended in either a 2D-DIC system [45] or a prism-based single-camera stereo-DIC system to achieve high-accuracy measurement, it is not generally applicable due to its fixed field of view, limited depth of focus and high cost.

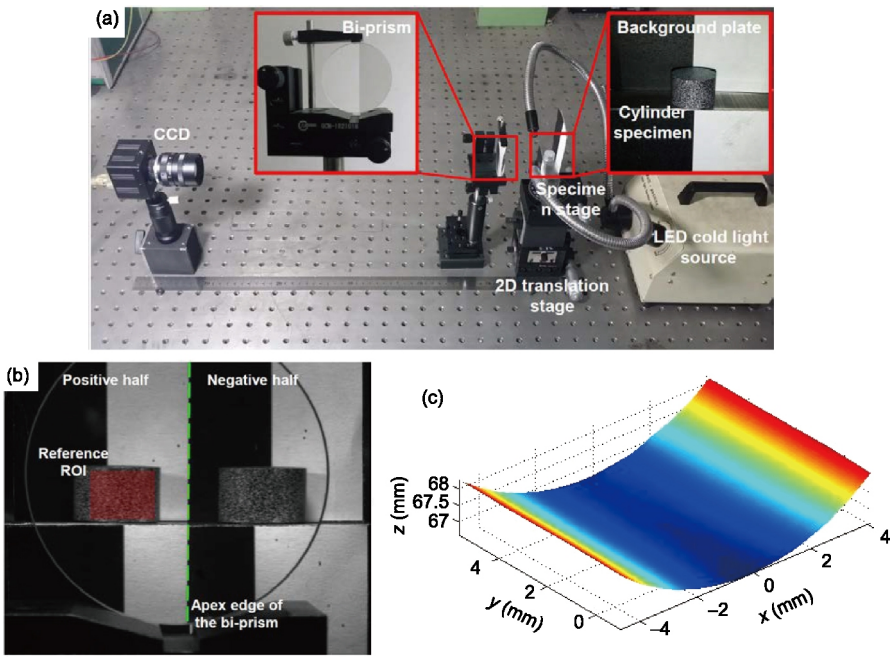

Figure 6 (Color online) (a) Experimental set-up for 3D shape measurement of a cylinder specimen using a single-camera stereo-DIC system with a bi-prism; (b) an image recorded to reconstruct the 3D shape; (c) retrieved 3D shape of the cylinder surface (Wu et al. [41]).

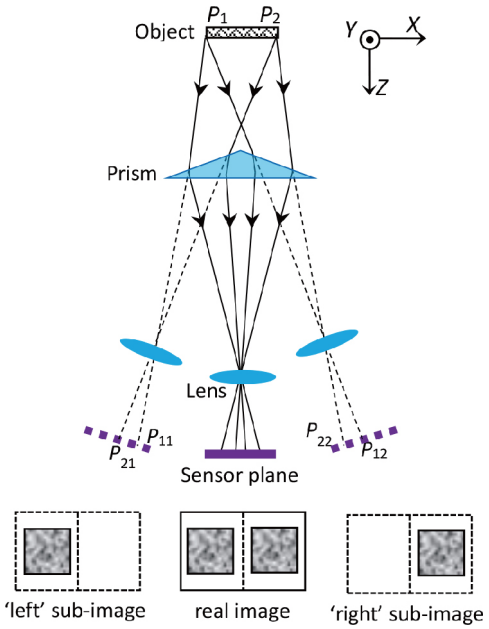

Figure 7 (Color online) Schematic diagram of the single-camera stereo-DIC system using a bi-prism and a conventional lens.

3.3 Principles

After surface images of the test object are recorded by using an established single-camera stereo-DIC system, obtained images can be processed to retrieve the 3D shape, motion and deformation on the object surface. However, additional unique distortion in the images is induced by placing a bi-prism in front of the camera, which cannot be adequately represented by existing distortion models and thus makes it difficult to calibrate or correct [36]. Therefore, numerous errors are incorporated into measuring results when using a conventional stereo-DIC algorithm, since the calibration model typically takes three major components of lens distortion (i.e., radial, decentering and thin prism distortions) into consideration.

To accurately determine the 3D information of the test object, two approaches are proposed in the literature. The first one does not depend upon prior knowledge of any parameters of the bi-prism, as presented by Genovese et al. [13]. A robust generalized stereo-system calibration framework was employed, which is insensitive to the camera and bi-prism misalignments, and a model-free optimization-based procedure was implemented to map and correct the image distortion error induced by the bi-prism over the entire measurement volume. Figure 8 shows the scheme of the optimization-based procedure for mapping and correcting the image distortion adopted by Genovese et al. [13]. By applying this procedure to the directly recorded images, the distortions caused by the nonlinear angle variation were eliminated. To accurately reconstruct 3D shape from each image of the different state, the captured images were first processed using a standard stereo-DIC algorithm and subsequently corrected using the proposed procedure. By subtracting the corrected 3D coordinates of the deformed stated from those of the initial state, 3D full-field displacement fields of different deformed

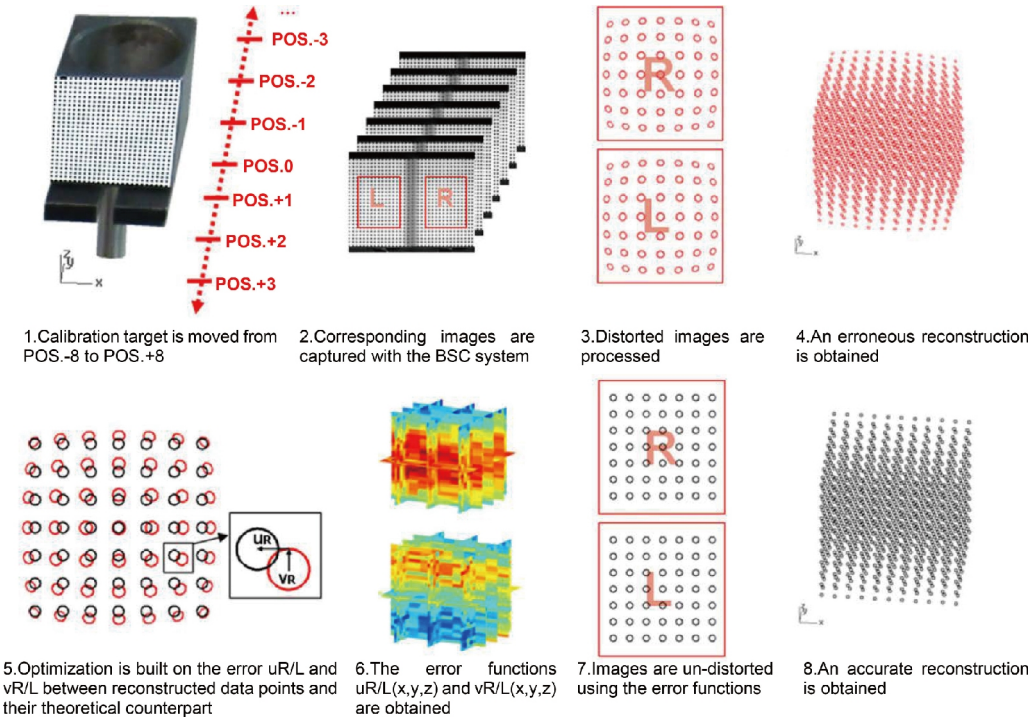

Figure 8 (Color online) Scheme of the optimization-based procedure for mapping and correcting the distortion error throughout the measurement volume (Genovese et al. [13]).

state can be obtained.

By contrast, a simplified calibration approach based on the backward ray-tracing method was adopted by Wu et al. [41]. Analogously to many prism-based single-camera stereovision systems, this approach needs a prior knowledge of the parameters of the bi-prism and thus greatly distinguishes from Genovese's approach. Figure 9(a) shows the imaging model of the single-camera stereo-DIC system using a bi-prism and a conventional lens. Based on the backward ray-tracing method and the pinhole imaging model, the spatial relations between the object point and virtual points, together with the mathematic relationships between the virtual points and their corresponding image coordinates, are first analyzed and derived. Then, for each image with two different views of the test object, the disparities between the left virtual points and right virtual points are calculated using a standard 2D-DIC algorithm. By rearranging the mathematic relationships with the disparities and then solving the equations using an iterative approach, the 3D coordinates of the object points can be retrieved. Similarly, the coordinates of the object points after deformation are also obtained by correlating the deformed image coordinates with the reference ones. Finally, 3D displacement components are determined by directly evaluating the coordinates' variations of these object points. More details about the derivations and iteration process are found in ref. [41].

In addition, Wu et al. [43] demonstrated a significant simplification in the reconstruction of the 3D coordinates after replacing the conventional pinhole-model-based lens by a bilateral telecentric lens. As presented in Figure 9(b), light rays are deflected from the original optical paths only at the front surface of the bi-prism, but directly pass through the interface without changing direction at the back surface. With this imaging model, the mathematical expressions between the virtual points and their corresponding image points are greatly reduced. After calculating the disparities of image points using 2D-DIC, the spatial coordinates of the corresponding object point are obtained by solving the mathematical equations. Similarly, by subtracting the deformed coordinates from the reference ones, the desired displacement components are obtained.

3.4 Systematic error calibration and correction

For prism-based single-camera stereo-DIC systems, the imaging lens and the bi-prism are the most important parts and usually supposed to be ideal in the imaging model. However, in practice, both the imaging lens and the bi-prism are not perfect and contain more or fewer deficiencies due to the manufacturing errors. Moreover, the misalignment between the camera and bi-prism will also affect the imaging model. Without a doubt, the shortcomings of the imaging device and the misalignment between the camera and bi-prism change the ideal imaging model and thus inevitably introduce errors

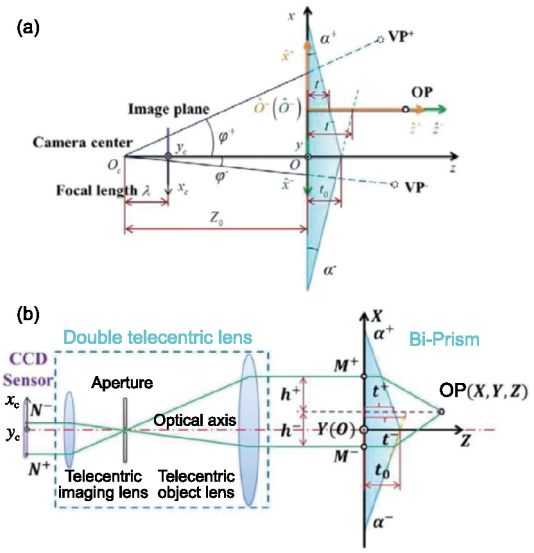

Figure 9 (Color online) Imaging models of the single-camera stereo-DIC system using a bi-prism and (a) a conventional lens (Wu et al. [41]) or (b) a bilateral telecentric lens (Wu et al. [43]).

into measuring results. To eliminate the errors caused by the imperfect imaging system and to achieve high-accuracy 3D shape and deformation measurement, the established bi-prism-based single-camera stereo-DIC system should be carefully calibrated.

In Genovese's work [13], since all kinds of distortions (including the distortion induced by the bi-prism and other distortions due to the imperfect imaging system) are corrected by the model-free calibration technique, an additional calibration is no longer required. However, for the simplified calibration approach [43], the deficiencies of the imaging system are not considered in the imaging models and thus should be carefully calibrated. A novel and practical shape retrieval method was proposed to improve the measurement precision [42]. In the modified approach, the light refractions in the bi-prism were considered in 3D space and the errors introduced by the imperfect imaging model was minimized by taking into account the misalignment between the bi-prism and the camera and the distortion of the lens.

4 Mirror-based single-camera stereo-DIC methods

4.1 Historical overview

In contrast to diffraction grating-based and bi-prism-based single-camera stereovision techniques, mirror-based single-camera stereovision techniques are more flexible on the system structure as it can be realized by combining a single camera with one or a set of mirrors. Zhang and Tsui [48] realized 3D reconstruction of objects using a single camera and a planar mirror. As shown in Figure 10(a) [49,50], with the aid of

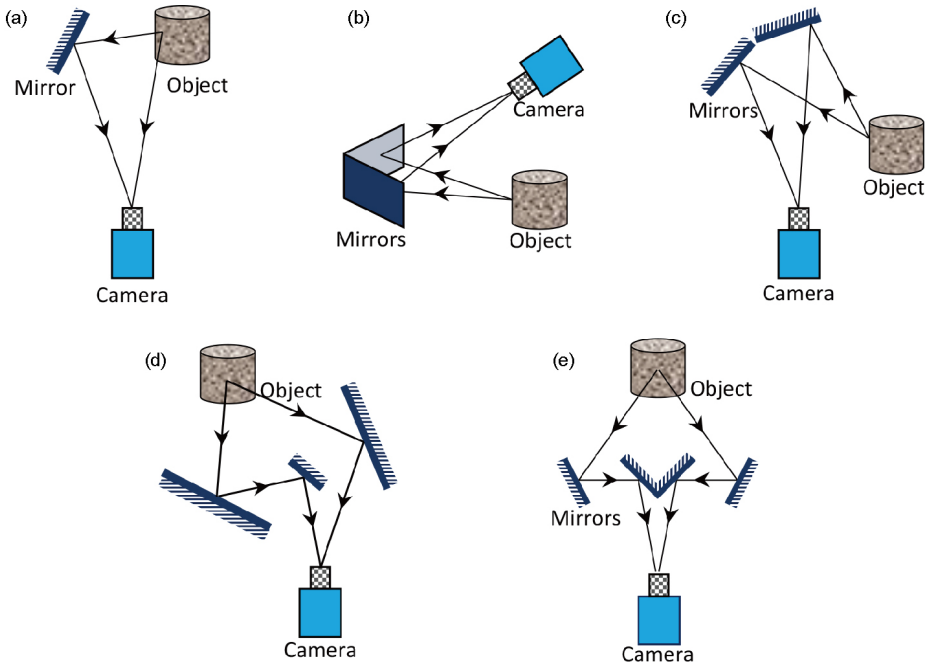

Figure 10 (Color online) Schematic diagram of the single-camera stereovision system using one mirror or a set of mirrors: (a) Zhang and Tsui [48]; (b) Goshtasby and Gruver [14]; (c) Gluckman and Nayar [49]; (d) Gluckman and Nayar [49]; (e) Inaba et al. [50].

a planar mirror, the object and its image in the mirror were both recorded by the camera. By processing these two images of the object using a 3D reconstruction algorithm, the shape information of the object was extracted. A similar approach was also adopted by Shaw et al. [51] to measure the full-field deformation of a plate under vibration. Feng and Pan [52] established the mathematical model of the single-camera stereo system using a planar mirror and analyzed its system parameters and accuracy. The obvious advantage of this system is its simplicity. However, the application of the system using one mirror is limited because the obvious optical path difference between the object and its image in the mirror, and may results in a blurred image if the depth of field of the camera is small. To prevent this problem, single-camera stereovision systems using a set of mirrors, instead of a single one, are investigated by various researchers. Goshtasby and Gruver [14] developed a single-camera stereovision system using two planar mirrors. Figure 10(b) shows that stereo image pair are achieved by viewing the reflections of the object in two mirrors that have a common axis. A similar stereovision system was established by Gluckman and Nayar [49], as shown in Figure 10(c). The geometry and calibration of the stereovision system with two planar mirrors were presented to show how the relative orientation, the epipolar geometry and the estimation of the focal length were constrained by the planar motion. Besides, Nene and Nayar [53] proposed single-camera stereovision techniques that use a single camera pointed toward planar, ellipsoidal, hyperboloidal, and paraboloidal mirrors. Although a wide field of view was obtained by using nonplanar reflecting surfaces, the calibration of these systems with curved mirrors is more complicated than those with planar mirrors.

The single-camera stereovision systems using three mirrors have been also developed. For example, as shown in Figure 10(d), Gluckman and Nayar [54,55] realized single-camera stereovision with the aid of three planar mirrors. These three mirrors were carefully designed and arranged with the appropriate size and location. A more flexible single-camera stereovision system using four mirrors was first established by Inaba et al. [50] as shown in Figure 10(e). Four planar mirrors were placed in front of the camera in a certain arrangement. With this four-mirror adapter, two views of the object surface via different optical reflection paths are imaged onto the sensor target of the camera. They carefully analyzed the optical structure of the single-camera stereo system and verified its effectiveness in stereo matching and 3D motion tracking as a stereo viewer of robots. Later, Seal et al. [56] also developed a similar structure for the depth perception and proved the system achieved a depth resolution of 5.8 cm at a working distance of 2 m. Additionally, a detailed analysis of the imaging model and in-depth discussion were performed by Wang et al. [57] and Zhu et al. [58]. Recently, more single-camera stereo imaging systems have been designed and devoted to a larger variety of applications, such as 3D geometry measurement of the flame surface [59,60], stereo-photography of streamers in the air [61] and feature parameters measurement of bubbles in gas [62,63]. Among the above mentioned mirror-based single-camera stereovision systems, the system using a four-mirror adapter is commonly preferred owing to its greater flexibility and

applicability.

In the DIC community, the mirror-based single-camera stereo-DIC system has been introduced for 3D shape and deformation measurements [12,64]. Compared with the diffraction grating-based and prism-based stereo-DIC systems, those using a four-mirror adapter not only measure the objects with larger size but also present negligible distortion caused by the additional optical device. Pankow et al. [12] established a single-camera stereo-DIC system, and successfully measured the out-of-plane deformations under a shock wave impact. Recently, the single-camera stereo-DIC system with a four-mirror adapter was optimized and thoroughly studied by the authors of this paper [65,66]. Specifically, to extend the application range and robustness of the single-camera stereo-DIC system, the novel idea of active imaging [46], which combines an actively illuminated monochromatic blue LED light source and a band-pass optical filter mounted just before the imaging lens, was compactly integrated to the established DIC system. Moreover, to get a clear knowledge of its optical model and further facilitate an optimal design of the optical structure for specific measurement objects, comprehensive analyses of the structure parameters, e.g., the baseline distance and valid field of view of the virtual stereo-DIC system, were conducted [66]. This method was further combined with a single high-speed camera for full-field 3D transient deformation measurements of carbon fiber reinforced polymer (CFRP) panels under impact loading [67] (Figure 11), full-field 3D vibration measurement [68], as well as the investigation of the formation of adiabatic shear bands [69]. With the aids of the properly arranged four-mirror adapter, the synchronization problem of two high-speed cameras can be automatically eliminated, enabling transient 3D deformation measurement through a single high-speed camera.

In addition, the four-mirror adapter assisted single-camera stereo-DIC system has also been designed to be compact, portable and miniaturized. For example, López-Alba et al. [70] established a portable single-camera stereo-DIC system that utilized a composite carbon fiber device to place the mirrors. Shao et al. [71] constructed a compact four-mirror adapter which used a triangular prism mirror and two exterior mirrors and was directly mounted onto the camera. In particular issues, Eisa et al. [72] established a miniature portable single-camera stereo-DIC system using a triangular prism mirror and two mirrors. Experimental results verified that the established system was practicable and efficient for the local 3D deformation measurement. To properly understand the single-camera stereo-DIC system using a four-mirror adapter, its system structure and principle are reviewed.

4.2 Optical arrangement

Figure 12 schematically shows experimental arrangements of the four-mirror adapter assisted single-camera stereo-DIC system [65]. The system consists of a single camera placed before the test object, a zoom lens mounted on the camera, a four-mirror adapter located between the test object and the camera. Note that the four-mirror adapter is composed of a perpendicular aluminum block, two mirror mounts, four

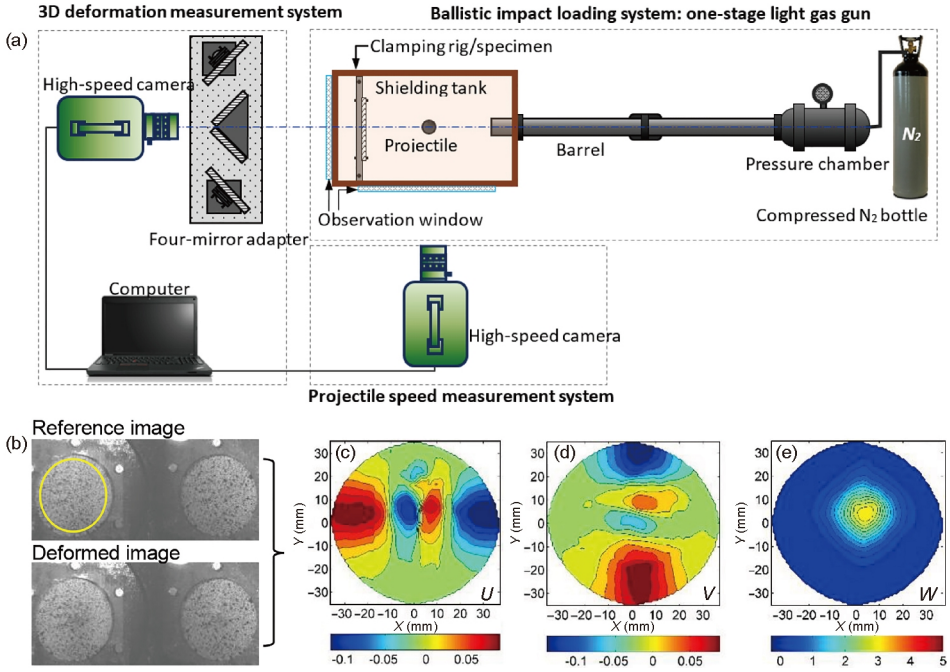

Figure 11 (Color online) (a) Schematic illustration of the experimental set-up for transient 3D deformation measurement under ballistic impact; (b) a reference image and a deformed image recorded before and during the test; Measured (c) U, (d) V and (e) W displacement fields on the back surface of the CFRP panel during the test (Pan et al. [68]).

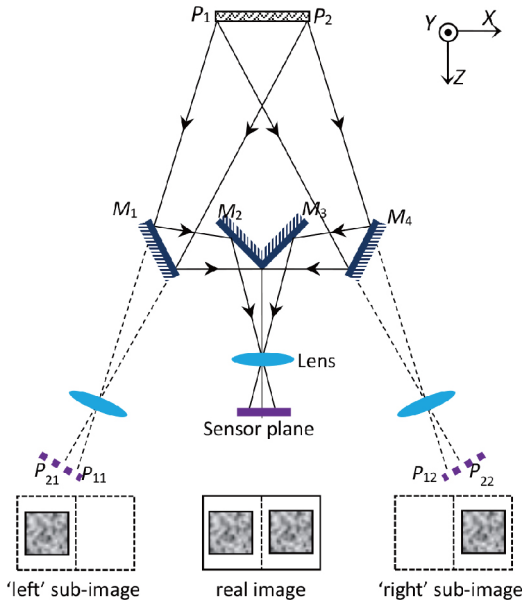

Figure 12 (Color online) Schematic diagram of the single-camera stereo-DIC system using a four-mirror adapter.

planar mirrors (denoted as M_1, M_2, M_3 and M_4, two inner planar mirrors can be replaced by a prism with two reflecting surfaces) and some fixed rods. Two interior mirrors are fixed on two sides of the perpendicular aluminum block and form a 90° angle with each other, while two exterior mirrors are glued tightly to mirror mounts and then mounted on rotating stages, which allows two exterior mirrors to rotate around their axes. The included angle between two interior mirrors is designed as any angle within a certain range. Then, by adjusting the posting angles of two exterior mirrors and the lens of the camera, two views of the test specimen surface via different optical reflection paths are projected onto two halves of the camera sensor target. The location and orientation of these two views on the recorded image are also finely tuned by adjusting mirror mounts.

4.3 Principles

Differing from the grating-based and prism-based single-camera stereo-DIC techniques, the additional image distortion induced by the planar mirrors is extremely small and even can be neglected. Thus, the recorded stereo image pairs can be processed to retrieve the 3D shape and deformation using the traditional stereo-DIC algorithm. Similarly, both calibration images of a calibration board and surface images of a test specimen are required to be captured during the experiment, as shown in Figure 13(a) and (b). As described in ref. [65], these images are segmented into two groups of left and right images, which only contain a single view of the calibration board or the test specimen with intensities of the other half image set as zero. The segmented images can be regarded as those recorded using a conventional two-camera stereo-DIC system and then are used to calculate the disparity data of the initial state and deformed states.

To accurately determine the disparity information required for 3D profile reconstruction, the well-developed subset-

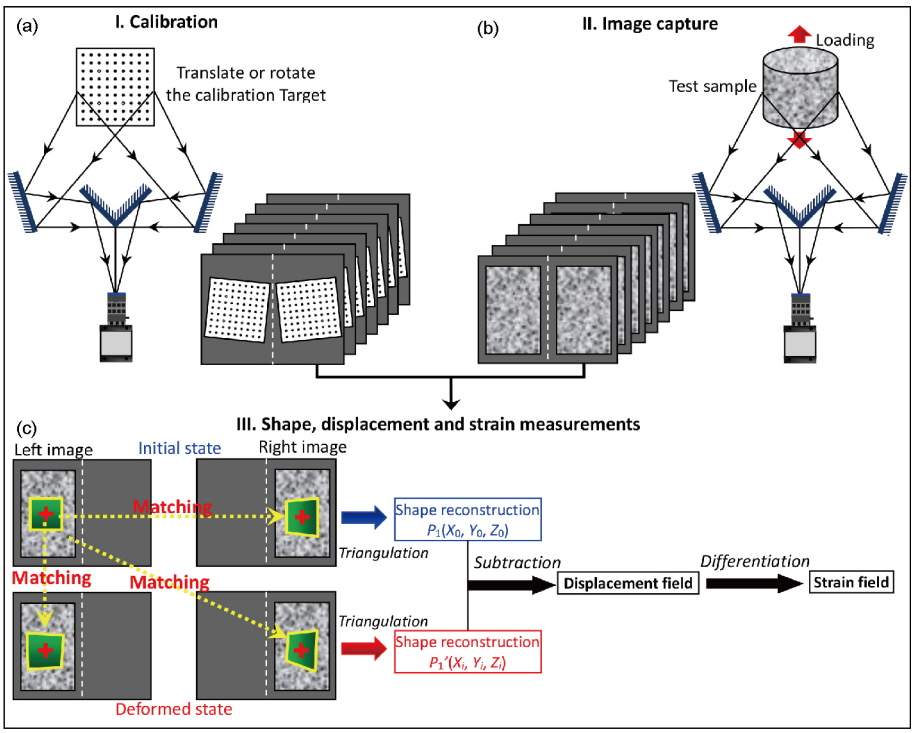

Figure 13 (Color online) Schematic showing the procedures for measuring 3D shape profile and deformation.

based DIC algorithm is utilized to accurately register the same physical points imaged in the left and right images. Specifically, a square subset centered at each predefined calculation point is selected from the left image of the initial state and used to search its target in the corresponding right one. To this purpose, a practical zero-mean normalized sum of squared difference criterion (ZNSSD) [73], combined with a second-order shape function, is utilized to quantitatively evaluate the similarity between the reference subsets and the target ones. By optimizing the nonlinear ZNSSD criterion using an inverse compositional Gauss-Newton (IC-GN) algorithm [74] and the bicubic spline interpolation scheme, the desired disparity data of the initial state are obtained. Finally, these disparity data, together with the previously determined calibration parameters, are used to reconstruct the profile of the ROI at initial state according to the triangulation principle. Similarly, the profile within the ROI after deformation can also be retrieved. By subtracting the 3D coordinates of the deformed stated from those of the initial state, 3D full-field displacement fields (i.e., U, V and W) of different deformed state can be obtained. It should be noted that this stereo-matching process is the same as the conventional stereo-DIC method using two cameras.

4.4 Calibration of the imaging system

As the distortion caused by the four-mirror adapter almost can be neglected, the only calibration needed for this single-camera stereo-DIC systems using a four-mirror adapter is to erect the world coordinate system of two virtual cameras, which is similar to the conventional stereovision calibration technique. The lens distortion is also considered in the calibration model.

According to the above understanding of the single-camera stereovision system, there exist two methods for the system calibration. The widely used one is referred as Respective Calibration Method, which considers the left and the right halves of the images captured by two different cameras as a traditional two-camera stereovision system [2,3]. Differing from this commonly used calibration method, the other approach was proposed based on the fact that the intrinsic parameters of two virtual cameras are theoretically identical. This method originally requires two steps for the calibration process. First, it needs to remove the mirror adapter, and then uses the single camera to capture the calibration target and to calibrate its fundamental parameters. After that, the mirrors adapter should be put back and the system is calibrated again using the target to determine structure parameters [75]. However, the structure parameters of the system may be slightly changed due to removing and recovering the mirrors during the calibration, and thus introducing additional artificial errors into the results. To address this problem, Zhou et al. [76] and Cui et al. [77] proposed a novel calibration method for the single-camera stereovision system using mirrors. This approach also considers intrinsic parameters of two virtual cameras as the same but does not need to remove the mirrors during the calibration.

5 Full-frame single-camera stereo-DIC using a color separation apparatus

As described above, the diffraction grating-based, biprism-based and mirror-based single-camera stereo-DIC systems enable 3D shape and deformation measurements using a single camera. It thus not only eliminates the synchronization problem of two cameras, but also leads to a cost-effective and compact experimental setup. However, as two or more views of the object are separately imaged on non-overlapped regions of one camera sensor, there are less than half the camera sensor available to define the region of interest (ROI), resulting in a substantial reduction in spatial resolution. For this reason, a single-camera stereo-DIC technique, which can make the most of the spatial resolution of the camera sensor, just like the regular binocular stereo-DIC system using two synchronized cameras, is highly desirable and undoubtedly exceptionally useful in practical applications.

Recently, the authors of this paper proposed a novel color stereo-DIC method using a single color camera for full-frame 3D shape, motion, and deformation measurements without any sacrifice of the camera sensor spatial resolution. In the first paper [16], a 3CCD color camera was adopted. With the aid of a skillfully designed color separation optical device, color images of a test sample surface can be readily divided into red and blue sub-images, which view the sample surface from two different orientations. The efficiency and accuracy of the color stereo-DIC method were successfully demonstrated by measuring the shape of a regular cylinder, in-plane and out-of-plane displacements of a translated plate and 3D deformation of a centrally loaded circular plastic plate.

Although the performances of 3CCD color cameras are better than conventional Bayer filter-based color CMOS cameras in color image separation, color CMOS cameras are more commonly used. In the second paper, this method was combined with a color high-speed camera, which was built with the CMOS sensor for high-speed deformation measurements [78]. As color crosstalk (also termed as color coupling or color contamination) problem unavoidably exists in the directly separated blue and red channel images, considerable errors will be introduced into the stereo-DIC measurement. To mitigate these errors induced by color crosstalk, Yu and Pan adopted a simple but effective color crosstalk correction method for the image correction [78]. Vibration responses measurement of a Chinese double-sided drum under the beating of a wood drumstick convincingly verified the effectiveness and accuracy of the single color CMOS camera-based stereo-DIC technique.

To validate the effectiveness and accuracy of the proposed single-camera stereo-DIC using a single 3CCD color camera

for 3D deformation measurement, 3D deformation measurements of a centrally loaded circular plastic plate were performed [16]. Figure 14 (a) shows the experimental set-up for 3D deformation measurements. During the test, the plastic plate was clamped all around the edge and loaded transverse to the center of the plate by means of a micrometer indenter installed behind the plate. Two images of the specimen surface were captured before and after deformation. These two images, together with the calibration images, were processed to retrieve the desired deformation according to the proposed approach. Figure 14(b)–(d) show the measured 3D full-field U, V, and W components of the surface deformation. The U displacement field presents an antisymmetric distribution with respect to the y axis, while the V displacement field shows an antisymmetric distribution on the x axis. Furthermore, the W displacement distributions present a perfect concentric pattern with the center located at the point of the applied load.

5.1 Optical arrangement

The optical arrangements of the established color stereo-DIC system are schematically illustrated in Figure 15. This system consists of a single color camera, a beam splitter prism placed before the camera lens, two optical bandpass filters with specific center wavelengths attached on the left and front of the beam splitter prism, and three planar mirrors (denoted as M_1, M_2 and M_3) arranged on the two optical paths. By adjusting the posting angles of the planar mirrors and the lens of the camera two views of the object surface can pass through the optical bandpass filters via two different optical paths and then enter into the sensor target of the color camera with the aid of the beam splitter. As a result, an overlapped color image composed of one blue color image and one red color image is directly captured. Compared with the single-camera stereovision systems using a biprism or a four-mirror adapter, it is obvious that this approach allows the left and right images to overlap each other in one image, which means the spatial resolution of the camera sensor can be fully utilized. The color images recorded at different configurations can be separated into red and blue channel sub-images, which correspond to the left and right images recorded by two virtual cameras. These separated images can be processed by regular stereo-DIC to retrieve the full-field 3D shape and deformation.

5.2 Image mechanisms and color crosstalk correction

Before the image separation and color crosstalk correction, it is desired to figure out the image mechanisms of the 3CCD and CMOS color cameras, which have been introduced in refs. [16,78]. As shown in Figure 16(a), a 3CCD color camera is composed of three separate charge-coupled devices with each one taking an independent measurement of the primary colors. After coming through the objective lens light rays are split by a trichroic prism assembly which directs the appropriate wavelength ranges of the light to their respective CCDs (https://en.wikipedia.org/wiki/Three-CCD_camera). Then images from all three image sensors are combined to form a color image. Figure 16(b) shows the quantum efficiencies of a 3CCD camera (AT-140CL, JAI Ltd., Japan) used in ref. [16]. The quantum efficiencies reflect the sensitivities of the camera sensor to incident light at different wavelengths. By placing blue and red optical bandpass

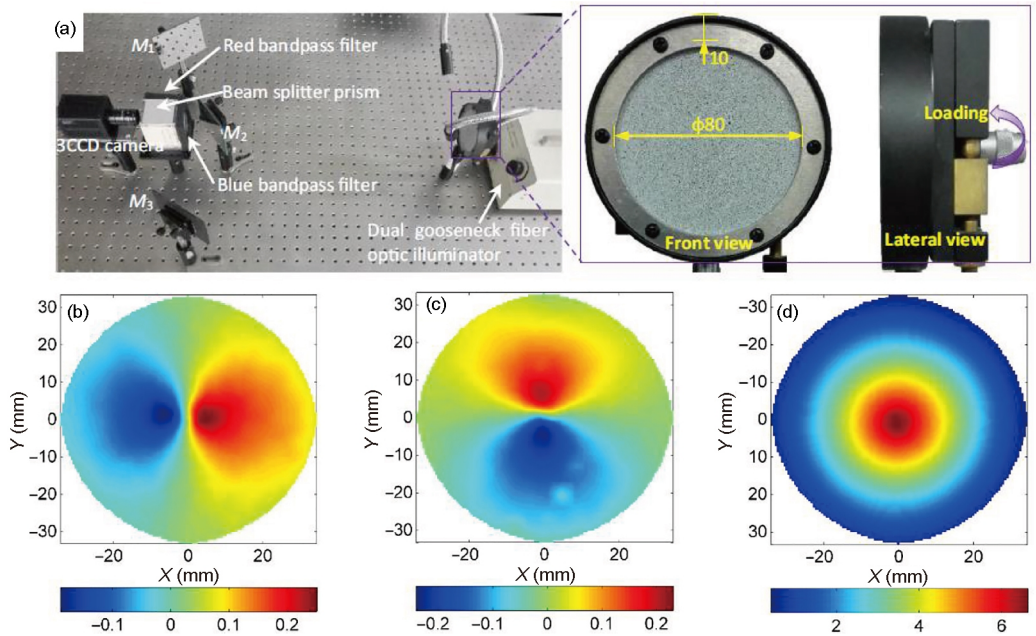

Figure 14 (Color online) 3D deformation measurements of a circular plastic plate subjected to a central load normal to the specimen surface: contour plots of the displacement components: (a) U, (b) V, and (c) W (Yu and Pan et al. [16]).

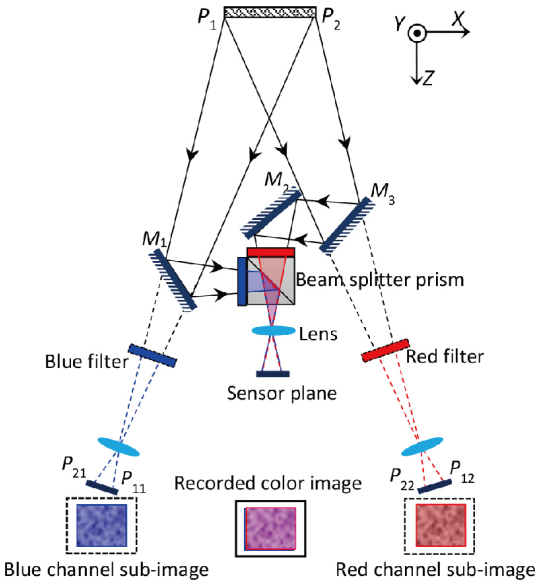

Figure 15 (Color online) Schematic diagram of the full-frame single-camera stereovision system using a color camera and three mirrors.

filters in two separate optical paths (Figure 15), only the light rays of specific wavelengths arrive at the corresponding camera sensor. There is no overlap between these two color channels, since blue and red channel sub-images from two different optical paths are thoroughly separated without mutual interference. This means that the directly separated red and blue channel sub-images are used for stereo matching without any correction.

By contrast, the imaging mechanism of the conventional CMOS color camera is somewhat complicated. As shown in Figure 16(c), a sequential pattern of red, green, and blue filters is arranged in a mosaic pattern and then mounted on the top of the imaging sensor pixel by pixel. As described in ref. [78], the demosaicing process results in overlapping spectra between each or neighboring channels. Figure 16(d) shows the quantum efficiency curves of the color high-speed camera (Y3C, Integrated Design Tools, Inc.) adopted in ref. [78]. Clearly, the spectral responses of red, green and blue are overlapped. These overlaps are undesirable because they cause color crosstalk problem in the separated color signals, and consequently bring considerable errors to DIC measurements. Therefore, for the color images recorded using a conventional CMOS color camera, it is necessary to remove the color crosstalk from the separated red and blue channel sub-images before stereo-DIC calculation.

In the recently proposed full-frame single-camera stereo-DIC method, an easily implemented and effective color correction method was applied by the authors and proven to be effective [78]. Note that this color correction method stemmed from color particle image velocimetry (PIV) [79,80], which uses multicolor illumination and a color camera. To remove the color crosstalk in separated sub-images, McPhail et al. [79] proposed a linear unmixing method which needs to determine crosstalk coefficient map by the color calibration. This method was also adopted by Wang et al. [80] in the triple-exposure color PIV technique. Differing from McPhail's work, a parabolic function is employed but not a linear one to describe the relationships among the intensity responses of R, G, B channel sub-images. It should be noted that using a parabolic function spends much more time than using a linear one due to massive requirements of nonlinear iterations for each pixel. However, for a high-speed

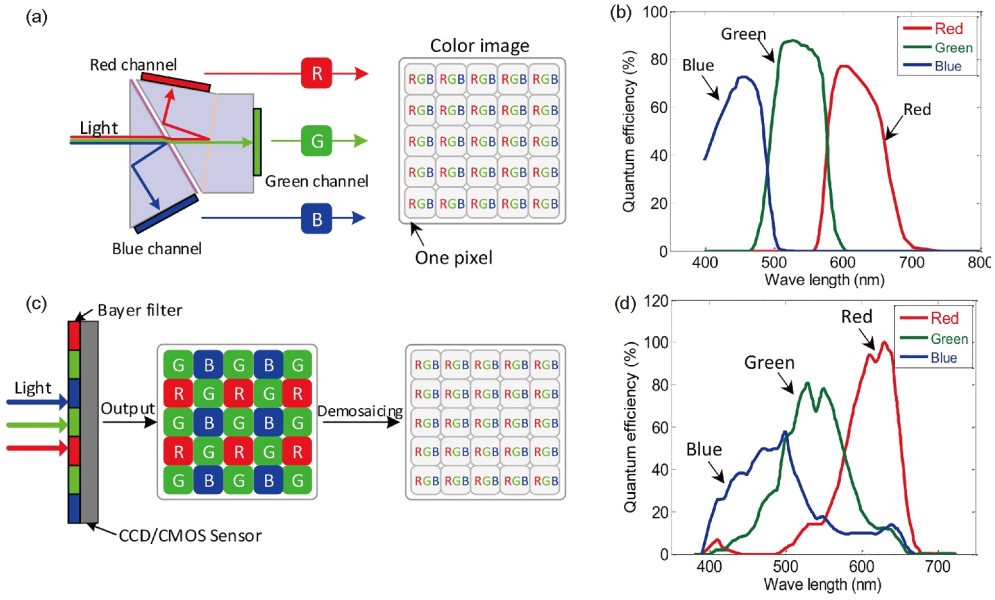

Figure 16 (Color online) Schematic diagrams of the imaging mechanisms for (a) 3CCD color camera and (c) conventional CMOS-based color camera with their quantum efficiency curves shown in (b) and (d).

test with thousands of images (e.g., 1 M pixel of each image), the time spending on the color crosstalk should be considered.

5.3 Principles

For the 3CCD camera, the separated image pair can be directly processed to retrieve the profile and deformation using the regular stereo-DIC algorithm, while those recorded using a conventional CMOS camera need a color crosstalk correction before stereo matching. After removing the color crosstalk, the corrected red and blue channel sub-images are used to retrieve the shape and deformation on the object surface using the regular stereo-DIC method. The principle of the proposed single-camera stereo-DIC method using a CMOS color camera is briefly described. First, a series of color images of a planar calibration target with regularly spaced circular dots, and surface images of the test specimen with premade speckle patterns are captured at different states using a color camera, respectively. Then, these recorded color images, including calibration images and experimental images, are separated into red and blue channel sub-images. Afterward, the separated sub-images are corrected using the color crosstalk correction method. Similar as the single-camera stereo-DIC technique using a four-mirror adapter, the well-developed subset-based DIC algorithm is used to accurately register the same physical points imaged in the corrected red and blue channel sub-images. Figure 17 shows a schematic of the procedure to measure the 3D shape and displacement. The stereo-matching and system calibration processes are not repeated herein, since they are similar to those used in the single-camera stereo-DIC using a four-mirror adapter.

6 Advantages and limitations of various single-camera stereo-DIC techniques

In the above sections, historical developments, optical configurations, basic principles, and typical applications of the diffraction grating-based, bi-prism-based, reflection mirror-based, and the newly presented full-frame single-camera stereo-DIC techniques are comprehensively reviewed. To properly understand the disadvantages, limitations and technical complexity of these technologies, Table 1 lists the key optical components, the size of available ROI, the size of

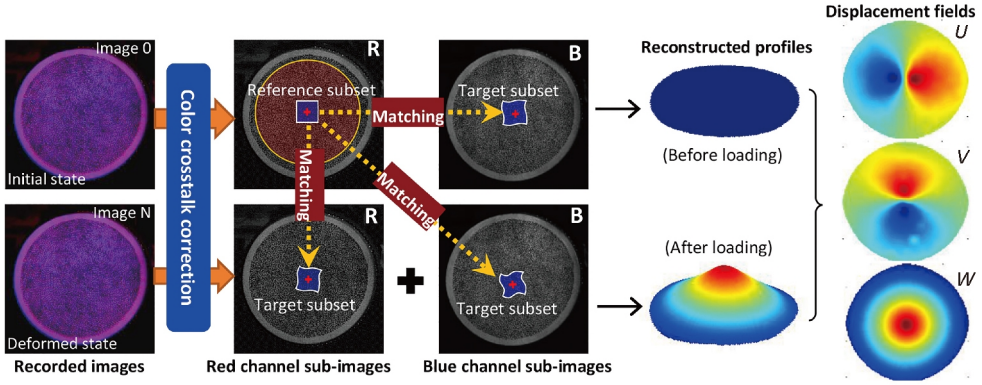

Figure 17 (Color online) The procedure to measure 3D shape profile and deformation.

Table 1 Comparisons of grating-based, prism-based, mirror-based and full-frame single-camera stereo-DIC techniques

Methods	Key component	Available ROI	Measuring object	Illumination	System calibration
Diffraction grating-based single-camera stereo-DIC	A diffraction grating	≤1/3 image	Small objects (sub-millimeters to a few centimeters)	Quasi-monochromatic source or white light source with bandpass optical filter mounted before lens	Magnification factor, the object distance and lens distortion
Prism-based single-camera stereo-DIC	A bi-prism	≤1/2 image	Limited by the bi-prism size and working distance	Quasi-monochromatic source or white light source with bandpass optical filter mounted before lens	Bi-prism distortion, lens distortion and misalignment between the camera and bi-prism
Mirror-based single-camera stereo-DIC	Four planar mirrors	≤1/2 image	Just as regular binocular stereo-DIC	Normal light source	Conventional stereo calibration
Full-frame single-camera stereo-DIC	A color separation apparatus and a color camera	≤full frame	Just as regular binocular stereo-DIC	Relatively strong light source (monochromatic supplementary light for certain camera)	Color crosstalk calibration and conventional stereo calibration

measuring object, the illumination source and the calibration techniques used in these four different kinds of single-camera stereo-DIC techniques. Compared with regular binocular stereo-DIC using two synchronized cameras, all these single-camera stereo-DIC techniques lead to a simpler, more compact and cost-effective optical configuration. However, it should be mentioned that diffraction grating-based and bi-prism-based single-camera stereo-DIC techniques are generally limited to small objects with a size of several sub-millimeter to dozens of millimeters. Otherwise, the overlap between diffracted or refracted images leads to decreased image quality. By comparison, the latter two single-camera stereo-DIC techniques used a four-mirror adaptor or a color separation apparatus seem to be more practical and promising, since they offer the same application range just like the conventional two-camera stereo-DIC technique does.

As far as the size of measuring object is concerned, we consider that diffraction grating-based single-camera stereo-DIC is suitable for 3D shape and deformation measurement of a single object with a size of sub- millimeters to a few centimeters. Prism-based ones can be applied to objects with slightly greater size, with special advantages for the cases with a small and deep optical window (e.g., a furnace) or using an endoscopic camera. The strengths of mirror-based, and the recently proposed full-frame single-camera stereo-DIC techniques are highly prominent in high-speed applications (e.g., transient deformation or dynamic testing) using a single high-speed camera.

7 Conclusions

Single-camera stereo-DIC methods have exceptional and attracting strengths over traditional stereo-DIC using two synchronized cameras, which have become an active research direction in recent several years. Diffraction grating-based, bi-prism-based and mirror-based single-camera stereo-DIC techniques have been successfully established by combing a diffraction grating, a bi-prism, a four-mirror adapter or a color separation apparatus with DIC, which has proven to be effective and accurate in numerous applications. This paper systematically reviews existing single-camera stereo-DIC techniques for full-field 3D shape and deformation measurements. The optical arrangements, basic principles and system calibrations of these single-camera stereo-DIC techniques are presented, and their strengths and limitations are discussed in detail. A brief comparison of grating-based, prism-based, mirror-based and full-frame single-camera stereo-DIC techniques are outlined. Since each technique has its strengths and weaknesses, an appropriate selection of optimal single-camera stereo-DIC should consider the size of the measurement object, experimental conditions and the simplicity of implementation.

More importantly, a single-camera high-speed (SCHS) stereo-DIC system can be easily achieved by replacing a conventional camera with a high-speed camera. The SCHS stereo-DIC system directly inherits all extraordinary merits of the standard single-camera stereo-DIC method. Compared with the common high-speed stereo-DIC system using two synchronized high-speed cameras, the hardware investment of an additional high-speed camera and synchronized and complicated techniques involved in the stringent camera synchronization are alleviated in the SCHS stereo-DIC system. Therefore, it demonstrates great potential in impact engineering, vibration and numerous dynamic tests.

This work was supported by the National Natural Science Foundation of China (Grant Nos. 11272032, 11322220, 11427802 & 11632010), the Aeronautical Science Foundation of China (Grant No. 2016ZD51034), and the Academic Excellence Foundation of BUAA for PhD Students.

1 Luo P F, Chao Y J, Sutton M A, et al. Accurate measurement of three-dimensional deformations in deformable and rigid bodies using computer vision. Exp Mech, 1993, 33: 123–132
2 Garcia D, Orteu J J, Penazzi L. A combined temporal tracking and stereo-correlation technique for accurate measurement of 3D displacements: Application to sheet metal forming. J Mater Process Tech, 2002, 125-126: 736–742
3 Pan B, Xie H M, Yang L H, et al. Accurate measurement of satellite antenna surface using 3D digital image correlation technique. Strain, 2009, 45: 194–200
4 Hu Z, Luo H, Du Y, et al. Fluorescent stereo microscopy for 3D surface profilometry and deformation mapping. Opt Express, 2013, 21: 11808–11818
5 Pan B, Wu D, Yu L. Optimization of a three-dimensional digital image correlation system for deformation measurements in extreme environments. Appl Optics, 2012, 51: 4409–4419
6 Tiwari V, Sutton M A, McNeill S R, et al. Application of 3D image correlation for full-field transient plate deformation measurements during blast loading. Int J Impact Eng, 2009, 36: 862–874
7 Helfrick M N, Niezrecki C, Avitabile P, et al. 3D digital image correlation methods for full-field vibration measurement. Mech Syst Signal Pr, 2011, 25: 917–927
8 Pan B, Qian K, Xie H, et al. Two-dimensional digital image correlation for in-plane displacement and strain measurement: A review. Meas Sci Technol, 2009, 20: 062001
9 Sutton M A, Yan J H, Tiwari V, et al. The effect of out-of-plane motion on 2D and 3D digital image correlation measurements. Opt Laser Eng, 2008, 46: 746–757
10 Pan B, Yu L, Wu D. High-accuracy 2D digital image correlation measurements with bilateral telecentric lenses: Error analysis and experimental verification. Exp Mech, 2013, 53: 1719–1733
11 Xing H Z, Zhang Q B, Braithwaite C H, et al. High-speed photography and digital optical measurement techniques for geomaterials: Fundamentals and applications. Rock Mech Rock Eng, 2017, 50: 1611–1659
12 Pankow M, Justusson B, Waas A M. Three-dimensional digital image correlation technique using single high-speed camera for measuring large out-of-plane displacements at high framing rates. Appl Optics, 2010, 49: 3418–3427
13 Genovese K, Casaletto L, Rayas J A, et al. Stereo-Digital Image Correlation (DIC) measurements with a single camera using a biprism. Opt Laser Eng, 2013, 51: 278–285
14 Goshtasby A, Gruver W A. Design of a single-lens stereo camera system. Pattern Recogn, 1993, 26: 923–937

15 Xia S, Gdoutou A, Ravichandran G. Diffraction assisted image correlation: A novel method for measuring three-dimensional deformation using two-dimensional digital image correlation. Exp Mech, 2013, 53: 755–765
16 Yu L, Pan B. Color stereo-digital image correlation method using a single 3CCD color camera. Exp Mech, 2017, 57: 649–657
17 Trivi M, Rabal H J. Stereoscopic uses of diffraction gratings. Appl Optics, 1988, 27: 1007–1009
18 Henao R, Medina F, Rabal H J, et al. Three-dimensional speckle measurements with a diffraction grating. Appl Optics, 1993, 32: 726–729
19 Rabal H, Henao R, Torroba R. Digital speckle pattern shearing interferometry using diffraction gratings. Optics Commun, 1996, 126: 191–196
20 Pan Z, Xia S, Gdoutou A, et al. Diffraction-assisted image correlation for three-dimensional surface profiling. Exp Mech, 2015, 55: 155–165
21 Pan B, Wang Q. Single-camera microscopic stereo digital image correlation using a diffraction grating. Opt Express, 2013, 21: 25056–25068
22 Pan B, Ma L J, Xia Y. A novel technique for measuring 3D deformation of adhesively bonded single lap joint. Sci China-Phys Mech Astron, 2016, 59: 614601
23 Xia S, Pan Z, Zhang J. Optical microscope for three-dimensional surface displacement and shape measurements at the microscale. Opt Lett, 2014, 39: 4267–4270
24 Lee D H, Kweon I S, Cipolla R. A biprism-stereo camera system. In: IEEE Computer Society Conference on Computer Vision and Pattern Recognition, 1999. IEEE, 1999, 1
25 Lee D H, Kweon I S. A novel stereo camera system by a biprism. IEEE Trans Robot Automat, 2000, 16: 528–541
26 Lim K B, Xiao Y. Virtual stereovision system: New understanding on single-lens stereovision using a biprism. J Electron Imag, 2005, 14: 043020
27 Cui X, Lim K B, Guo Q, et al. Accurate geometrical optics model for single-lens stereovision system using a prism. J Opt Soc Am A, 2012, 29: 1828–1837
28 Kee W L, Lim K B, Tun Z L, et al. New understanding on the effects of angle and position of biprism on single-lens biprism stereovision system. J Electron Imag, 2014, 23: 033005
29 Cui X, Zhao Y, Lim K, et al. Perspective projection model for prism-based stereovision. Opt Express, 2015, 23: 27542–27557
30 Kee W L, Bai Y, Lim K B. Parameter error analysis of single-lens prism-based stereovision system. J Opt Soc Am A, 2015, 32: 367–373
31 Lim K B, Kee W L, Wang D. Virtual camera calibration and stereo correspondence of single-lens bi-prism stereovision system using geometrical approach. Signal Process-Image, 2013, 28: 1059–1071
32 Zhao M, Lim K B, Kee W L. Geometrical-analysis-based algorithm for stereo matching of single-lens binocular and multi-ocular stereovision system. J Electron Sci Technol, 2012, 10: 107–112
33 Kee W L, Lim K B, Wang D L. Virtual epipolar line construction of single-lens bi-prism stereovision system. J Electron Sci Tech, 2012, 10: 97–101
34 Qian B, Lim K B. Image distortion correction for single-lens stereo vision system employing a biprism. J Electron Imag, 2016, 25: 043024
35 Deng Q L, Chen C Y, Cheng S W, et al. Micro-prism type single-lens 3D aircraft telescope system. Optics Commun, 2012, 285: 5001–5007
36 Lim K B, Qian B. Biprism distortion modeling and calibration for a single-lens stereovision system. J Opt Soc Am A, 2016, 33: 2213–2224
37 Xiao Y, Lim K B. A prism-based single-lens stereovision system: From trinocular to multi-ocular. Image Vision Comput, 2007, 25: 1725–1736
38 Wang D, Lim K B, Kee W L. Geometrical approach for rectification of single-lens stereovision system with a triprism. Machine Vision Appl, 2013, 24: 821–833
39 Chen C Y, Yang T T, Sun W S. Optics system design applying a microprism array of a single lens stereo image pair. Opt Express, 2008, 16: 15495–15505
40 Yang S P, Kim J J, Jang K W, et al. Compact stereo endoscopic camera using microprism arrays. Opt Lett, 2016, 41: 1285–1288
41 Wu L, Zhu J, Xie H. A modified virtual point model of the 3D DIC technique using a single camera and a bi-prism. Meas Sci Technol, 2014, 25: 115008
42 Wu L F, Zhu J G, Xie H M, et al. An accurate method for shape retrieval and displacement measurement using bi-prism-based single lens 3D digital image correlation. Exp Mech, 2016, 56: 1611–1624
43 Wu L, Zhu J, Xie H. Single-lens 3D digital image correlation system based on a bilateral telecentric lens and a bi-prism: Validation and application. Appl Optics, 2015, 54: 7842–7850
44 Wu L, Zhu J, Xie H, et al. Single-lens 3D digital image correlation system based on a bilateral telecentric lens and a bi-prism: Systematic error analysis and correction. Opt Laser Eng, 2016, 87: 129–138
45 Pan B, Wu D F, Wang Z Y, et al. High-temperature digital image correlation method for full-field deformation measurement at 1200°C. Meas Sci Technol, 2011, 22: 015701
46 Pan B, Wu D F, Xia Y. An active imaging digital image correlation method for deformation measurement insensitive to ambient light. Optics Laser Tech, 2012, 44: 204–209
47 Wu L F, Yin Y J, Zhang Q, et al. Bi-prism-based single lens three dimensional digital image correlation (BSL 3D DIC) system with long working distance: Methodology and application in extreme high temperature deformation test. Sci China Tech Sci, doi: 10.1007/s11431-017-9082-3
48 Zhang Z Y, Tsui H T. 3D reconstruction from a single view of an object and its image in a plane mirror. In: Proceedings Fourteenth International Conference on Pattern Recognition, 1998. Brisbane, 1998. 2: 1174–1176
49 Gluckman J, Nayar S K. Planar catadioptric stereo: Geometry and calibration. In: IEEE Computer Society Conference on Computer Vision and Pattern Recognition, 1999. Fort Collins, 1999. 1: 22–28
50 Inaba M, Hara T, Inoue H. A stereo viewer based on a single camera with view-control mechanisms. In: Proceedings of the 1993 IEEE/RSJ International Conference on Intelligent Robots and Systems'93, IROS'93. Yokohama, 1993. 3: 1857–1865
51 Shaw A D, Neild S A, Wagg D J, et al. Single source three dimensional capture of full field plate vibrations. Exp Mech, 2012, 52: 965–974
52 Feng X, Pan D. Research on the application of single camera stereo vision sensor in three-dimensional point measurement. J Modern Opt, 2015, 62: 1204–1210
53 Nene S A, Nayar S K. Stereo with mirrors. In: Sixth International Conference on Computer Vision, 1998. Bombay, 1998. 1087–1094
54 Gluckman J, Nayar S K. Catadioptric stereo using planar mirrors. Int J Comp Vision, 2001, 44: 65–79
55 Gluckman J, Nayar S K. Rectified catadioptric stereo sensors. IEEE Trans Pattern Anal Machine Intell, 2002, 24: 224–236
56 Seal J R, Bailey D G, Gupta G S. Depth perception with a single camera. In: Proceedings of International Conference on Sensing Technology. Palmerston North, 2005. 96–101
57 Wang R, Li X, Zhang Y. Analysis and optimization of the stereo-system with a four-mirror adapter. J Eur Opt Soc: Rapid Publ, 2008, 3: 08033
58 Zhu J, Li Y, Ye S. Design and calibration of a single-camera-based stereo vision sensor. Opt Eng, 2006, 45: 083001
59 Ng W B, Zhang Y. Stereoscopic imaging and reconstruction of the 3D geometry of flame surfaces. Exp Fluids, 2003, 34: 484–493
60 Ng W B, Zhang Y. Stereoscopic imaging and computer vision of impinging fires by a single camera with a stereo adapter. Int J Imag Syst Technol, 2005, 15: 114–122
61 Nijdam S, Moerman J S, Briels T M P, et al. Stereo-photography of

streamers in air. Appl Phys Lett, 2008, 92: 101502
62 Xue T, Qu L, Cao Z, et al. Three-dimensional feature parameters measurement of bubbles in gas-liquid two-phase flow based on virtual stereo vision. Flow Meas Instrum, 2012, 27: 29–36
63 Xue T, Qu L, Wu B. Matching and 3-D reconstruction of multibubbles based on virtual stereo vision. IEEE Trans Instrum Meas, 2014, 63: 1639–1647
64 Besnard G, Lagrange J M, Hild F, et al. Characterization of necking phenomena in high-speed experiments by using a single camera. EURASIP J Image Video Process, 2010, 2010: 1–15
65 Yu L, Pan B. Single-camera stereo-digital image correlation with a four-mirror adapter: Optimized design and validation. Opt Laser Eng, 2016, 87: 120–128
66 Yu L, Pan B. Structure parameter analysis and uncertainty evaluation for single-camera stereo-digital image correlation with a four-mirror adapter. Appl Optics, 2016, 55: 6936–6946
67 Pan B, Yu L, Yang Y, et al. Full-field transient 3D deformation measurement of 3D braided composite panels during ballistic impact using single-camera high-speed stereo-digital image correlation. Compos Struct, 2016, 157: 25–32
68 Yu L, Pan B. Single-camera high-speed stereo-digital image correlation for full-field vibration measurement. Mech Syst Signal Pr, 2017, 94: 374–383
69 White T G, Patten J R W, Wan K H, et al. A single camera three-dimensional digital image correlation system for the study of adiabatic shear bands. Strain, 2017, 53: e12226
70 López-Alba E, Felipe-Sesé L, Schmeer S, et al. Optical low-cost and portable arrangement for full field 3D displacement measurement using a single camera. Meas Sci Technol, 2016, 27: 115901
71 Shao X, Eisa M M, Chen Z, et al. Self-calibration single-lens 3D video extensometer for high-accuracy and real-time strain measurement. Opt Express, 2016, 24: 30124–30138
72 Eisa M M, Shao X X, He X Y. Portable device for local three-dimensional deformation measurement using a single camera (in press). Sci China Tech Sci,
73 Pan B, Xie H, Wang Z. Equivalence of digital image correlation criteria for pattern matching. Appl Optics, 2010, 49: 5501–5509
74 Pan B, Li K, Tong W. Fast, robust and accurate digital image correlation calculation without redundant computations. Exp Mech, 2013, 53: 1277–1289
75 Zhu J, Yang J, Li Y, et al. Study on structure precision of single camera stereo vision measurement. Sci Tech Eng, 2007, 17: 8
76 Zhou F, Wang Y, Peng B, et al. A novel way of understanding for calibrating stereo vision sensor constructed by a single camera and mirrors. Measurement, 2013, 46: 1147–1160
77 Cui Y, Zhou F, Wang Y, et al. Precise calibration of binocular vision system used for vision measurement. Opt Express, 2014, 22: 9134–9149
78 Yu L, Pan B. Full-frame, high-speed 3D shape and deformation measurements using stereo-digital image correlation and a single color high-speed camera. Opt Laser Eng, 2017, 95: 17–25
79 McPhail M J, Fontaine A A, Krane M H, et al. Correcting for color crosstalk and chromatic aberration in multicolor particle shadow velocimetry. Meas Sci Technol, 2015, 26: 025302
80 Wang Z Y, Gao Q, Wang J J. A triple-exposure color PIV technique for pressure reconstruction. Sci China Tech Sci, 2017, 60: 1–15